MycoKeys 117: 337–352 (2025)
DOI: 10.3897/mycokeys.117.151366

Research Article

Phylogenetic evidence reveal a close relationship between *Amphichorda* and *Ovicillium* in Bionectriaceae (Hypocreales)

Yao Wang[1,2], De-Xiang Tang[1,2], Hui Chen[1,2], Qi-Rui Li[1,2], Chanhom Loinheuang[3], Xiang-Chun Shen[1,2]

1 *The High Efficacy Application of Natural Medicinal Resources Engineering Center of Guizhou Province, Guizhou Medical University, Guian New District, Guizhou 561113, China*
2 *State Key Laboratory of Discovery and Utilization of Functional Components in Traditional Chinese Medicine & School of Pharmaceutical Sciences, Guizhou Medical University, Guian New District, Guizhou 561113, China*
3 *Department of Biology, Faculty of Natural Sciences, National University of Laos, Vientiane 01080, Laos*

Corresponding authors: Yao Wang (wangyao1@aliyun.com); Xiang-Chun Shen (shenxiangchun@126.com)

Abstract

Animal excrement serves as the primary substrate for *Amphichorda*, which is found in a wide range of habitats. Based on evolutionary relationships, the genus is currently classified within the Bionectriaceae. However, the phylogenetic position of *Amphichorda* and its associated taxa remains unresolved due to limited sampling in previous studies. Here, we discovered and identified five *Amphichorda* species, significantly advancing our understanding of this genus. Using six genomic loci (ITS, nrSSU, nrLSU, *tef1α*, *rpb1*, and *rpb2*) to expand taxonomic sampling, we reconstructed a phylogenetic framework for the Bionectriaceae, with a focus on *Amphichorda* and related taxa. Phylogenetic analyses revealed a close genetic connection between *Amphichorda* and related genera, yet they formed distinct clades within the Bionectriaceae and were clearly differentiated. The extensive sampling demonstrated stable phylogenetic relationships among *Amphichorda*, *Hapsidospora*, *Ovicillium*, *Proxiovicillium*, and *Bulbithecium*. Furthermore, we described two new species, *A. guizhouensis* **sp. nov.** and *O. pseudoattenuatum* **sp. nov.**, supported by DNA data and morphological characteristics. A comprehensive comparison of morphological traits across all members of *Amphichorda* and *Ovicillium* was conducted. This study clarifies taxonomic boundaries and evolutionary relationships within the two genera and contributes to the overall understanding of the biodiversity and systematics of the Bionectriaceae.

Key words: Coprophilous fungi, morphology, multi-locus phylogeny, new taxa, soil fungi, taxonomy

OPEN ACCESS

This article is part of:
Exploring the Hidden Fungal Diversity: Biodiversity, Taxonomy, and Phylogeny of Saprobic Fungi
Edited by Samantha C. Karunarathna, Danushka Sandaruwan Tennakoon, Ajay Kumar Gautam

Academic editor:
Danushka Sandaruwan Tennakoon
Received: 25 February 2025
Accepted: 17 April 2025
Published: 15 May 2025

Citation: Wang Y, Tang D-X, Chen H, Li Q-R, Loinheuang C, Shen X-C (2025) Phylogenetic evidence reveal a close relationship between *Amphichorda* and *Ovicillium* in Bionectriaceae (Hypocreales). MycoKeys 117: 337–352. https://doi.org/10.3897/mycokeys.117.151366

Copyright: © Yao Wang et al.
This is an open access article distributed under terms of the Creative Commons Attribution License (Attribution 4.0 International – CC BY 4.0).

Introduction

Renowned researcher E.M. Fries created the genus *Amphichorda* in 1825, designating *Amphichorda felina* (DC.) Fr. as the type species. The fungus, isolated from cat feces, was characterized by filiform conidiogenous cells and colonies with a white farinaceous hue (Fries 1825). Subsequently, Fries (1832) transferred *A. felina* to the genus *Isaria* Pers., and de Hoog (1972) formally designated *Isaria felina* (DC.) Fr. as the lectotype of the genus,

following von Arx's criteria derived from synnemata production. Based on the morphological similarity of the holoblastic conidiogenous cells, *I. felina* was accommodated in the genus *Beauveria* Vuill. as *B. felina* (DC.) J.W. Carmich. (Carmichael et al. 1980). Aside from its normal conidiogenous cells without an elongated denticulate rachis, *Amphichorda* shares a morphological resemblance with *Beauveria* (Rehner et al. 2011; Chen et al. 2013). However, phylogenetic analyses in previous studies revealed significant differences between *B. felina* and other *Beauveria* species (Hodge et al. 2005). Therefore, the genus *Amphichorda* has been reestablished with *B. felina* based on the phylogenetic relationships of internal transcribed spacer (ITS) sequences and morphology (Zhang et al. 2017). A phylogenetic analysis revealed that *Amphichorda* species were grouped in a separate clade from *Beauveria* sensu stricto, indicating the significant phylogenetic separation between the two taxa (Zhang et al. 2017). Further studies by Zhang et al. (2017, 2020) and Liu et al. (2023) placed *Amphichorda* within Cordycipitaceae and described three new species in the genus. Through a phylogenetic analysis based on a concatenated alignment of the ITS and nuclear ribosomal large subunit (nr*LSU*) sequences of Bionectriaceae and Cordycipitaceae, Guerra-Mateo et al. (2023) identified *Amphichorda* as a member of the Bionectriaceae family and established its close phylogenetic link to *Hapsidospora* Malloch & Cain and *Nigrosabulum* Malloch & Cain. Hou et al. (2023) determined that *Nigrosabulum* and *Hapsidospora* are congeneric, leading to their synonymization within Bionectriaceae based on both phylogeny and morphology. Leão et al. (2024) and Wang et al. (2024) also supported the placement of *Amphichorda* in the Bionectriaceae family. Despite these numerous studies, the evolutionary connections between *Amphichorda* and other genera remain unclear. It is imperative to reconstruct the phylogenetic framework for the Bionectriaceae focusing on *Amphichorda* through more sampling.

Animal excrement serves as the primary substrate for *Amphichorda*, which are found in a wide range of habitats. Currently, nine *Amphichorda* species viz. *A. cavernicola*, *A. coprophila*, *A. excrementa*, *A. felina*, *A. guana*, *A. kunmingensis*, *A. littoralis*, *A. monjolensis*, and *A. yunnanensis* have been published in reputable mycological journals (Zhang et al. 2017, 2020; Liu et al. 2023; Guerra-Mateo et al. 2023; Leão et al. 2024; Wang et al. 2024). The majority of the species are coprophilous (such as *A. coprophila*, *A. excrementa*, *A. guana*, and *A. kunmingensis*); some species are both coprophilous and entomopathogenic (such as *A. cavernicola* and *A. felina*); and one species was isolated from marine sediments (*A. littoralis*), other species from the wing surfaces of *Rhinolophus affinis* or *Rhinolophus siamensis* (*A. yunnanensis*), or a potato dextrose agar plate partially consumed by an insect (*A. monjolensis*) (Zhang et al. 2017, 2020; Liu et al. 2023; Guerra-Mateo et al. 2023; Leão et al. 2024; Wang et al. 2024).

During an extensive mycological survey conducted in two distinct biogeographical regions spanning China and Laos, seven fungal species were isolated from diverse ecological niches, including soil substrates and animal fecal matter. To complement field-collected specimens, reference strains from the Westerdijk Fungal Biodiversity Institute's CBS culture collection were incorporated into the study. A multilocus phylogenetic reconstruction integrating ITS, the nuclear ribosomal small subunit (nrSSU),

nrLSU, the translation elongation factor 1α (*tef1α*), the largest subunit of RNA polymerase II (*rpb1*), and the second subunit of RNA polymerase II (*rpb2*) sequences confirmed their taxonomic placement within Bionectriaceae. Among these taxa, two novel species, one belonging to the genus *Amphichorda* and the other to *Ovicillium* Zare & W. Gams, were proposed and described based on morphological traits and multi-locus molecular phylogenetic data. The morphological features of every component of *Amphichorda* and *Ovicillium* were also compared in detail. In addition to introducing and characterizing these two new species, the study aimed to: (1) re-evaluate the taxonomic stability of *Amphichorda* among related genera within Bionectriaceae, (2) delineate the taxonomic boundaries and evolutionary relationships within *Amphichorda* and *Ovicillium* through comparative morphological analysis, and (3) enhance the phylogenetic resolution within Bionectriaceae using six genomic loci.

Materials and methods

Isolates

The samples were collected from three locations: Anshun City, China; Vientiane City, Laos; and Muang Xay District, Oudomxay Province, Laos. The techniques outlined in Wang et al. (2023) were used to isolate the strains from the soil and animal feces. Briefly, 2 g of soil was added to a flask containing 20 mL sterilized water and glass beads. The soil suspension was shaken for about 10 min and then diluted 100 times. Subsequently, 200 µL of the diluted soil suspension was spread on Petri dishes with solidified onion garlic agar (OGA: 20 g of grated garlic and 20 g of onion were boiled in 1 L of distilled water for 1 h; the boiled residue was then filtered off, and 2% (w/v) agar was added to the filtrate). Czapek yeast extract agar (CYA, Advanced Technology and Industrial Co., Ltd., China) and potato dextrose agar (PDA, Difco, USA) were used, and all media had 50 mg/L rose Bengal and 100 mg/L kanamycin added. Conidia developing on animal feces were transplanted onto plates of PDA and cultured at 25 °C. Colonies of the isolated filamentous fungi appearing in the culture were transferred onto fresh PDA media. The purified fungal strain was transferred to PDA slants and cultured at 25 °C until its hyphae spread across the entire slope. The emerging fungal spores were washed with sterile physiological saline and made into a spore suspension of 1 × 103 cells/mL. To obtain monospore cultures, a part of the spore suspension was placed on PDA using a sterile micropipette, and then a Petri dish was incubated at 25 °C. Specimens and type material were deposited in the Guizhou Medical University Herbarium (GMB), China. Living cultures were deposited at the Guizhou Medical University Culture Collection (GMBC). This investigation comprised a total of nine isolates, including species that were tentatively classified as belonging to allied genera, *Amphichorda*, and *Ovicillium* (Table 1). Cultures of four *Amphichorda* species were acquired from the CBS-KNAW Fungal Biodiversity Centre (CBS, Westerdijk Fungal Biodiversity Institute, WI, Utrecht, the Netherlands). Following transfer to PDA medium, the CBS strains were re-cultured.

Table 1. Species information and corresponding GenBank accession numbers of *Amphichorda* and close relative genera used in this study.

Species	Strain	Genbank accession number						Reference
		ITS	nr*SSU*	nr*LSU*	*tef1α*	*rpb1*	*rpb2*	
Acremonium acutatum	CBS 682.71^{T}	OQ429438	N/A	OQ055349	OQ470735	N/A	OQ453833	Hou et al. 2023
Acremonium alternatum	CBS 407.66^{T}	OQ429442	N/A	OQ055353	OQ470739	N/A	OQ560696	Hou et al. 2023
Acremonium chlamydosporium	CBS 414.76^{T}	OQ429450	N/A	OQ055361	OQ470748	N/A	OQ453844	Hou et al. 2023
Acremonium cf. *egyptiacum*	CBS 270.86	OQ429463	N/A	OQ055374	OQ470760	N/A	OQ453857	Hou et al. 2023
Acremonium egyptiacum	CBS 114785^{T}	OQ429456	N/A	OQ055362	OQ470749	N/A	OQ453845	Hou et al. 2023
Alloacremonium ferrugineum	CBS 102877^{T}	OQ429495	N/A	OQ055406	OQ470785	N/A	OQ453887	Hou et al. 2023
Alloacremonium humicola	CBS 613.82^{T}	OQ429496	N/A	OQ055407	OQ470786	N/A	OQ453888	Hou et al. 2023
Amphichorda cavernicola	CGMCC 3.19571^{T}	MK329056	N/A	MK328961	MK335997	N/A	N/A	Zhang et al. 2020
Amphichorda cavernicola	LC12481	MK329057	N/A	MK328962	MK335998	N/A	N/A	Zhang et al. 2020
Amphichorda cavernicola	LC12560	MK329061	N/A	MK328966	MK336002	N/A	N/A	Zhang et al. 2020
Amphichorda coprophila	**CBS 173.71**	**PQ726811**	**PQ726824**	**PQ726836**	**PQ758601**	N/A	**PQ779067**	**This study**
Amphichorda coprophila	CBS 247.82^{T}	MH861494	N/A	MH873238	OQ954487	N/A	N/A	Guerra-Mateo et al. 2023
Amphichorda coprophila	CBS 424.88	OQ942929	N/A	OQ943166	OQ954488	N/A	N/A	Guerra-Mateo et al. 2023
Amphichorda excrementa	YFCC AECCS848^{T}	N/A	OR913433	OR913439	OR917446	OR917451	OR917443	Wang et al. 2024
Amphichorda excrementa	**CBS 110.08**	**PQ726812**	**PQ726825**	**PQ726837**	**PQ758602**	**PQ758614**	**PQ779068**	**This study**
Amphichorda feline	**CBS 250.34**	**PQ726813**	**PQ726826**	**PQ726838**	**PQ758603**	**PQ758615**	**PQ779069**	**This study**
Amphichorda feline	CBS 648.66	OQ942930	N/A	MH870575	OQ954491	N/A	N/A	Guerra-Mateo et al. 2023
Amphichorda guana	CGMCC3.17908^{T}	KU746665	KY883262	KU746711	KX855211	KY883202	KY883228	Zhang et al. 2017
Amphichorda guana	CGMCC3.17909	KU746666	KY883263	KU746712	KX855212	KY883203	N/A	Zhang et al. 2017
Amphichorda guizhouensis	**GMBC 3005^{T}**	**PQ726815**	**PQ726828**	**PQ726840**	**PQ758605**	**PQ758617**	**PQ779071**	**This study**
Amphichorda guizhouensis	**GMBC 3006**	**PQ726816**	**PQ726829**	**PQ726841**	**PQ758606**	**PQ758618**	**PQ779072**	**This study**
Amphichorda kunmingensis	YFCC AKYYH8414^{T}	N/A	OR913435	OR913438	OR917448	OR917452	N/A	Wang et al. 2024
Amphichorda kunmingensis	**CBS 312.50**	**PQ726814**	**PQ726827**	**PQ726839**	**PQ758604**	**PQ758616**	**PQ779070**	**This study**
Amphichorda littoralis	FMR 17952	OQ942925	N/A	OQ943162	OQ954483	N/A	N/A	Guerra-Mateo et al. 2023
Amphichorda littoralis	FMR 19404^{T}	OQ942924	N/A	OQ943161	OQ954482	N/A	N/A	Guerra-Mateo et al. 2023
Amphichorda littoralis	FMR 19611	OQ942926	N/A	OQ943163	OQ954484	N/A	N/A	Guerra-Mateo et al. 2023
Amphichorda monjolensis	COAD 3124^{T}	OQ288256	N/A	OQ288260	OR454090	N/A	OQ405040	Leão et al. 2024
Amphichorda monjolensis	COAD 3125	OQ288257	N/A	N/A	N/A	N/A	OQ405041	Leão et al. 2024
Amphichorda monjolensis	COAD 3120	OQ288258	N/A	N/A	N/A	N/A	OQ405042	Leão et al. 2024
Amphichorda yunnanensis	KUMCC 21-0414	ON426823	N/A	N/A	OR025977	OR022016	OR022041	Liu et al. 2023
Amphichorda yunnanensis	KUMCC 21-0415	ON426824	N/A	N/A	OR025976	OR022015	OR022040	Liu et al. 2023
Amphichorda yunnanensis	KUMCC 21-0416^{T}	ON426825	N/A	N/A	OR025975	OR022014	OR022039	Liu et al. 2023
Bulbithecium ammophilae	CBS 178.78^{T}	OQ429504	N/A	OQ055415	OQ470793	N/A	OQ453895	Hou et al. 2023
Bulbithecium arxii	CBS 737.84^{T}	OQ429505	N/A	OQ055416	OQ470794	N/A	OQ451834	Hou et al. 2023
Bulbithecium borodinense	CBS 101148^{T}	OQ429506	N/A	OQ055417	OQ470795	N/A		Hou et al. 2023
Bulbithecium ellipsoideum	CBS 993.69^{T}	OQ429507	N/A	OQ055418	OQ470796	N/A	OQ453896	Hou et al. 2023
Bulbithecium hyalosporum	CBS 318.91^{T}	OQ429508	AF096172	OQ055419	OQ470797	N/A	OQ453897	Hou et al. 2023
Bulbithecium pinkertoniae	CBS 157.70^{T}	OQ429509	HQ232202	OQ055420	OQ470799	N/A	OQ453898	Hou et al. 2023
Bulbithecium spinosum	CBS 136.33^{T}	OQ429512	HQ232210	OQ055423	OQ470802	N/A	OQ453899	Hou et al. 2023
Bulbithecium truncatum	CBS 113718^{T}	OQ429513	N/A	OQ055424	OQ470803	N/A	OQ453900	Hou et al. 2023
Claviceps paspali	ATCC 13892	JN049818	U32401	U47826	DQ522321	DQ522367	DQ522416	Spatafora et al. 2007
Claviceps purpurea	SA cp11	N/A	EF469122	EF469075	EF469058	EF469087	EF469105	Sung et al. 2007

Species	Strain	Genbank accession number						Reference
		ITS	nr*SSU*	nr*LSU*	*tef1α*	*rpb1*	*rpb2*	
Clonostachys kunmingensis	**GMBC 3002**	**PQ726821**	**PQ726833**	**PQ726846**	**PQ758611**	N/A	**PQ758622**	**This study**
Clonostachys rosea	**GMBC 3003**	**PQ726822**	**PQ726834**	**PQ726847**	**PQ758612**	**PQ779065**	**PQ779076**	**This study**
Clonostachys solani	**GMBC 3004**	**PQ726823**	**PQ726835**	**PQ726848**	**PQ758613**	**PQ779066**	**PQ779077**	**This study**
Geosmithia lavendula	CBS 344.48^{T}	OQ429598	N/A	OQ055508	OQ470908	N/A	OQ453997	Hou et al. 2023
Geosmithia pallidum	CBS 260.33^{T}	OQ429599	N/A	OQ055509	OQ470909	N/A	OQ453998	Hou et al. 2023
Hapsidospora chrysogena	CBS 144.62^{T}	OQ429645	HQ232187	OQ055551	OQ470953	N/A	OQ454043	Hou et al. 2023
Hapsidospora flava	CBS 596.70^{T}	OQ429649	HQ232191	OQ055555	OQ470957	N/A	OQ454047	Hou et al. 2023
Hapsidospora globosa	CBS 512.70^{T}	OQ429655	N/A	OQ055561	OQ470963	N/A	OQ454053	Hou et al. 2023
Hapsidospora inversa	CBS 517.70^{T}	OQ429659	N/A	OQ055565	OQ470967	N/A	OQ454057	Hou et al. 2023
Hapsidospora irregularis	CBS 510.70^{T}	OQ429660	N/A	OQ055566	OQ470968	N/A	OQ454058	Hou et al. 2023
Hapsidospora stercoraria	CBS 516.70^{T}	OQ429662	N/A	OQ055568	OQ470970	N/A	OQ454060	Hou et al. 2023
Hapsidospora variabilis	CBS 100549^{T}	OQ429663	N/A	OQ055569	OQ470971	N/A	OQ454061	Hou et al. 2023
Ovicillium asperulatum	CBS 426.95	KU382192	N/A	KU382233	OQ471081	N/A	OQ454166	Hou et al. 2023
Ovicillium asperulatum	CBS 130362^{T}	OQ429756	N/A	OQ055655	OQ471082	N/A	OQ454167	Hou et al. 2023
Ovicillium attenuatum	CBS 399.86^{T}	OQ429757	N/A	OQ055656	OQ471083	N/A	OQ454168	Hou et al. 2023
Ovicillium oosporum	CBS 110151^{T}	OQ429758	N/A	OQ055657	OQ471084	N/A	OQ454169	Hou et al. 2023
Ovicillium pseudoattenuatum	**GMBC 3007^{T}**	**PQ726817**	**PQ726830**	**PQ726842**	**PQ758607**	**PQ779063**	**PQ779073**	**This study**
Ovicillium pseudoattenuatum	**GMBC 3008**	**PQ726818**	**PQ726831**	**PQ726843**	**PQ758608**	**PQ779064**	**PQ779074**	**This study**
Ovicillium sinense	SD09701^{T}	PP836762	N/A	PP836764	PP852887	N/A	N/A	Chen et al. 2024
Ovicillium sinense	SD09702	PP836763	N/A	PP836765	PP852888	N/A	N/A	Chen et al. 2024
Ovicillium subglobosum	CBS 101963^{T}	OQ429759	N/A	OQ055658	OQ471085	N/A	OQ454170	Hou et al. 2023
Ovicillium variecolor	CBS 130360^{T}	OQ429760	N/A	OQ055659	OQ471086	N/A	OQ454171	Hou et al. 2023
Proxiovicillium blochii	CBS 324.33	OQ429815	N/A	OQ430078	OQ471143	N/A	OQ454212	Hou et al. 2023
Proxiovicillium blochii	CBS 427.93^{T}	OQ429816	HQ232182	OQ430079	OQ471144	N/A	OQ454213	Hou et al. 2023
Proxiovicillium lepidopterorum	CBS 101239^{T}	OQ429817	N/A	OQ430080	OQ471145	N/A	OQ454214	Hou et al. 2023
Proliferophialis apiculata	CBS 303.64^{T}	OQ429796	N/A	OQ055692	OQ471122	N/A	OQ454207	Hou et al. 2023
Proliferophialis apiculata	CBS 397.78	OQ429798	N/A	OQ055694	OQ471124	N/A	OQ454209	Hou et al. 2023
Proliferophialis apiculata	CBS 542.79	OQ429799	N/A	OQ055695	OQ471125	N/A	OQ454210	Hou et al. 2023
Sesquicillium buxi	**GMBC 3000**	**PQ726819**	N/A	**PQ726844**	**PQ758609**	**PQ758619**	**PQ758621**	**This study**
Sesquicillium candelabrum	**GMBC 3001**	**PQ726820**	**PQ726832**	**PQ726845**	**PQ758610**	**PQ758620**	**PQ779075**	**This study**
Stilbocrea colubrensis	CBS 141857^{T}	MN497406	N/A	MN497409	N/A	N/A	N/A	Lechat and Fournier 2019
Stilbocrea macrostoma	CBS 141849	OQ429874	N/A	OQ430123	OQ471206	N/A	OQ454273	Hou et al. 2023
Stilbocrea walteri	CBS 144627^{T}	OR050519	N/A	OQ430124	MH562714	N/A	MH577042	Voglmayr and Jaklitsch 2019
Waltergamsia moroccensis	CBS 512.82^{T}	OQ429943	N/A	OQ430193	OQ471276	N/A	OQ454343	Hou et al. 2023
Waltergamsia parva	CBS 381.70A^{T}	OQ429946	N/A	OQ430196	OQ471279	N/A	OQ454346	Hou et al. 2023
Waltergamsia pilosa	CBS 124.70^{T}	OQ429949	N/A	OQ430199	OQ471282	N/A	OQ454349	Hou et al. 2023

Morphological observations

After seven days (for *Ovicillium* species) or thirty days (for *Amphichorda* species) in an incubator set at 25 °C, colonies on potato dextrose agar (PDA) were macroscopically described. Characteristics and colony diameters were measured after 7 or 30 days. To take pictures of the colony characters (upper surface and reverse), a Canon 750 D camera (Canon Inc., Tokyo, Japan) was used. Colonies with micromorphological characteristics were seen at 25 °C on PDA. A light microscope (Olympus BX53) was used to examine the micro-morphological features (Conidiophores, Phialides, and Conidia) using sterile water or clear lactophenol cotton blue solution as the mounting medium.

DNA extraction, amplification and sequencing

Axenic cultures grown on PDA plates for 14 days were used for DNA extraction. The CTAB approach, as outlined by Liu et al. (2001), was used to extract genomic DNA. The ITS, nrSSU, nrLSU, *tef1α*, *rpb1*, and *rpb2* were amplified. For the PCR amplification of six genes, the following primer pairs were employed: The ITS region was amplified using the primer combination ITS5/ITS4 (White et al. 1990). The primer pairs NS1/NS4 and LR0R/LR5 were amplified for the nrSSU region and the nrLSU region (Vilgalys and Hester 1990; White et al. 1990; Hopple 1994); the primer pairs 2218R/983F, RPB1-5'F/RPB1-5'R and RPB2-5'F/RPB2-5'R were amplified for the *tef1α* region, the *rpb1* region and the *rpb2* region (Rehner and Buckley 2005; Bischoff et al. 2006; Sung et al. 2007). The polymerase chain reaction (PCR) matrix was conducted in a final volume of 50 µl and all detailed information (volume, procedures, etc.) was described by Wang et al. (2023). The consensus sequences were generated by aligning forward and reverse sequencing reads with Geneious Prime 2022 (Biomatters Inc., New Zealand).

Phylogenetic analyses

GenBank provided newly generated sequencing data (http://blast.ncbi.nlm.nih.gov/ (accessed on 20 February 2025)). The sequences mainly referred to recent articles, such as Zhang et al. (2020), Guerra-Mateo et al. (2023) and Hou et al. (2023). MAFFT v. 7 (https://mafft.cbrc.jp/alignment/server/ (accessed on 20 February 2025)) was used to create the sequence alignments for the six distinct loci (ITS, nrSSU, nrLSU, *tef1α*, *rpb1*, and *rpb2*). Where required, the aligned sequences were subsequently manually adjusted. The concatenated alignments (nrSSU + ITS + nrLSU + *tef1α* + *rpb1* + *rpb2*) were subjected to phylogenetic inferences using the maximum-likelihood (ML) and the Bayesian inference (BI) methods. IQ-tree v.2.1.3 and RAxML7.0.3 were used to conduct ML analyses using 1000 bootstrap replicates and the default general time reversible (GTR) substitution matrix (Stamatakis et al. 2008; Minh et al. 2020). ModelFinder was used to estimate the best evolutionary model for machine learning analyses (Kalyaanamoorthy et al. 2017). The TN+F+I+G4 model was selected as the optimal model for the ML analyses, with 5000 ultrafast bootstraps in a single run (Hoang et al. 2017). jModeltest v. 2.1.4 was used to estimate the optimal substitution model for Bayesian analysis and then performed using MrBayes v. 3.2.6 to assess posterior probabilities (PP) by Markov Chain Monte Carlo sampling (MCMC). For all loci in Bayesian analysis, the GTR+I+G model was suggested based on the results of jModeltest (Darriba et al. 2012; Ronquist et al. 2012). For 3,000,000 generations, four Markov chains ran simultaneously, sampling trees every 1000th generations or until the average standard deviation of split frequencies fell below 0.01 to trigger an automated stop. Following the first 25% of trees being removed as part of the burn-in phase, the posterior probabilities (PP) were computed from the remaining trees. The generated trees were annotated in Microsoft PowerPoint and displayed in FigTree v. 1.4.2 (http://tree.bio.ed.ac.uk/software/figtree (accessed on 20

February 2025)). Each node of the tree displays the ML bootstrap support values (BS) greater than or equal to 80% and the relevant Bayesian posterior probability (PP) more than or equal to 0.90.

Results

Molecular phylogeny

Relevant sequences of 65 strains from GenBank were used in the phylogenetic analyses. The aim was to estimate the phylogeny of *Amphichorda* and its closely related taxa within the Bionectriaceae family. *Claviceps paspali* (ATCC 13892) and *Claviceps purpurea* (SA cp11) were designated as outgroup taxa for the analyses. Six concatenated loci (nrSSU + ITS + nrLSU + *tef1α* + *rpb1* + *rpb2*) were utilized to analyze the aligned DNA sequence data of 78 strains, as presented in Table 1. The final dataset consisted of 6,509 bp of sequence data, including gaps (nrSSU, 2,012 bp; ITS, 705 bp; nrLSU, 906 bp; *tef1α*, 995 bp; *rpb1*, 756 bp; and *rpb2*, 1,135 bp). Overall, the maximum likelihood (ML) trees generated by IQ-TREE and RAxML exhibited the same clades and tree structure as those obtained from the Bayesian phylogenetic analysis. With the bootstrap support values of the ML analysis (IQ-TREE-BS/RAxML-BS) and pertinent Bayesian posterior probabilities (PP) displayed at the nodes (Fig. 1), the optimal IQ-TREE tree based on the combined dataset was displayed here.

Fourteen well-supported clades were recognized based on both ML and BI analyses of the 78 taxa from Bionectriaceae and *Claviceps* (Clavicipitaceae, Hypocreales) that accommodate species of the genera *Acremonium*, *Alloacremonium*, *Amphichorda*, *Bulbithecium*, *Clonostachys*, *Geosmithia*, *Hapsidospora*, *Ovicillium*, *Proxiovicillium*, *Proliferophialis*, *Sesquicillium*, *Stilbocrea*, *Waltergamsia*, and *Claviceps* (Fig. 1). The phylogenetic analyses clearly indicated that *Amphichorda* was a monophyletic group, suggesting a common evolutionary origin. The genus *Amphichorda* had a close genetic relationship with *Hapsidospora* and *Ovicillium*, but they were clearly distinguished from their allied genera by forming three separate clades within the Bionectriaceae family. In the phylogenetic tree, the genera *Proxiovicillium* and *Bulbithecium* were also closely related to *Amphichorda*.

In this study, 13 fungal isolates were examined, including four CBS strains. The results showed that these isolates represented nine known species and two new species. The phylogenetic positions of the nine known species were evaluated according to phylogenetic inferences based on the six loci, including *Amphichorda coprophila*, *A. excrementa*, *A. felina*, *A. kunmingensis*, *Clonostachys kunmingensis*, *C. rosea*, *C. solani*, *Sesquicillium buxi*, and *S. candelabrum* (see Table 1, Fig. 1). The phylogenetic analyses also resolved most *Amphichorda* and *Ovicillium* lineages in separate terminal branches. It was proposed that two strains, GMBC 3005 and GMBC 3006, which formed a distinct lineage and had a close relationship with *A. felina* and *A. yunnanensis*, might be a new species in the genus *Amphichorda*, named *A. guizhouensis*. Our analyses further revealed that the newly discovered species, *O. pseudoattenuatum* (GMBC 3007 and GMBC 3008), were phylogenetically clustered with *O. attenuatum* and *O. sinense*, but it was clearly distinguished from the latter two species by forming a well-supported clade in the genus *Ovicillium* (BS_{IQ}/BS_{RAx}/PP = 82%/-/0.93; Fig. 1).

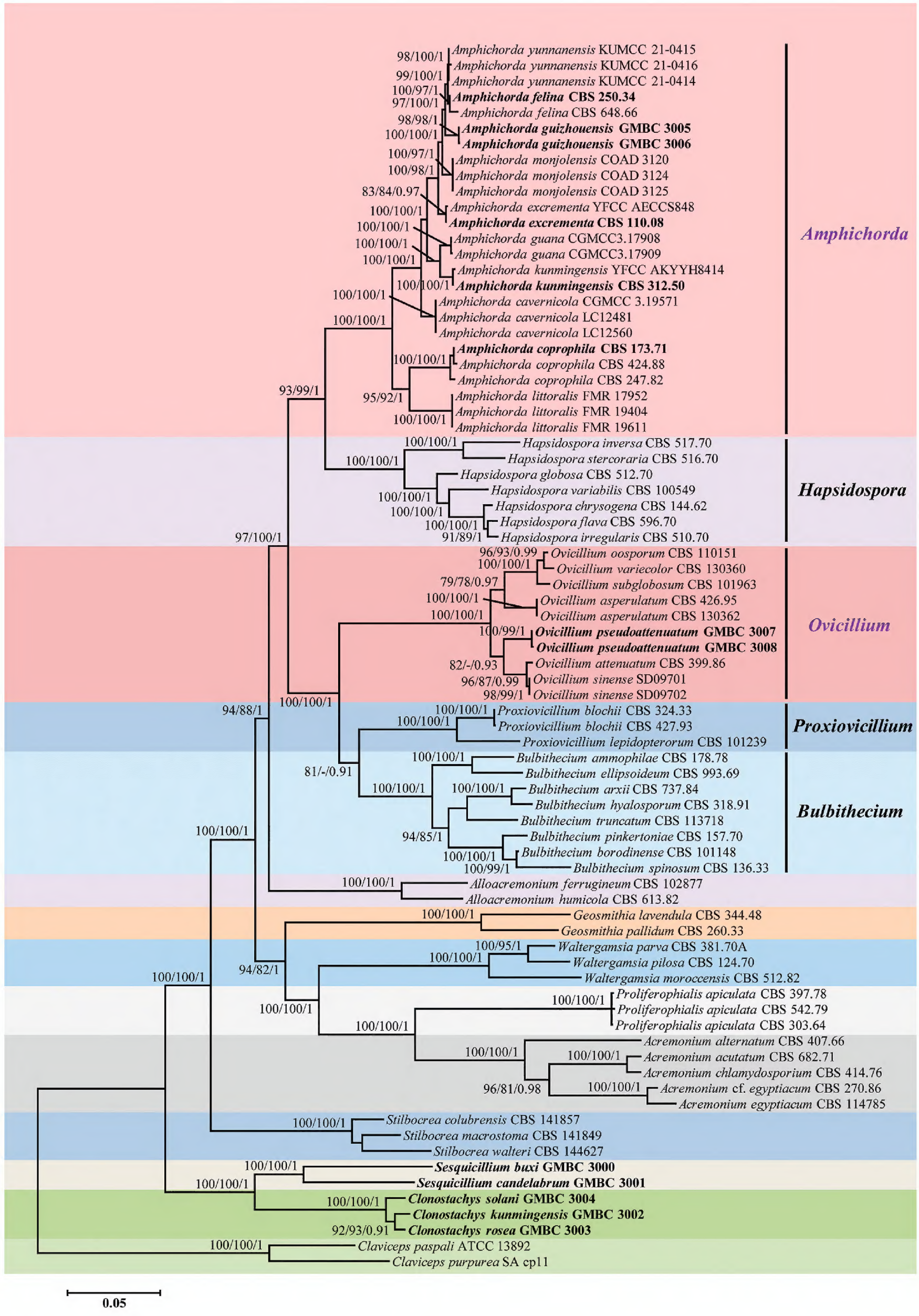

Figure 1. Phylogenetic relationships of *Amphichorda* and related genera in the Bionectriaceae based on combined partial nrSSU + ITS + nrLSU + *tef1α* + *rpb1* + *rpb2* sequences. Numbers at the nodes are presented here with ML bootstrap support values (BS) (IQ-TREE-BS_{IQ} > 80%/RAxML-BS_{RAx} > 80%) and relevant Bayesian posterior probabilities (PP) (PP > 0.90). Strains in bold type are those analyzed in this study.

Taxonomy

***Amphichorda guizhouensis* Y. Wang & D.X. Tang, sp. nov.**
MycoBank No: 857725
Fig. 2

Etymology. Named after the location Guizhou Province where the species was collected.

Type. China • Guizhou Province, Anshun city, Xixiu District, Liuguan Village (26.25°N, 106.22°E, 1273 m above sea level), on bird feces, 12 July 2023, Yao Wang (holotype, GMB 3005); ex-type culture, GMBC 3005.

Description. Sexual morph: Undetermined. **Asexual morph: *Synnemata*** arising from bird feces, 1.6–2.0 mm long. Colonies on PDA attaining a diameter of 40–42 mm after a month at 25 °C, white to pinkish, flat, margin entire, reverse yellowish. ***Hyphae*** branched, smooth-walled, septate, hyaline, 0.8–2.2 µm wide. ***Conidiophores*** arising laterally from hyphae, cylindrical, straight or slightly curved, occasionally branched, hyaline. ***Conidiogenous cells*** arising laterally from aerial hyphae, basal portion cylindrical or flask-shaped, erect or irregularly curved, tapering abruptly towards the apex, 6.0–20.8 × 1.8–3.7 ($\bar{X}$ = 15.2 × 2.6, n = 30) µm. ***Conidia*** 2.6–4.0 × 1.8–2.6 ($\bar{X}$ = 3.1 × 2.2, n = 50) µm, one-celled, smooth-walled, hyaline, subglobose to ellipsoidal, single, often remaining attached to the apex of conidiogenous cells. ***Chlamydospores*** not observed.

Other material examined. China • Guizhou Province, Anshun City, Xixiu District, Liuguan Village (26.25°N, 106.22°E, 1269 m above sea level), on bird feces, 12 July 2023, Yao Wang (paratype: GMB 3006); ex-paratype culture, GMBC 3006).

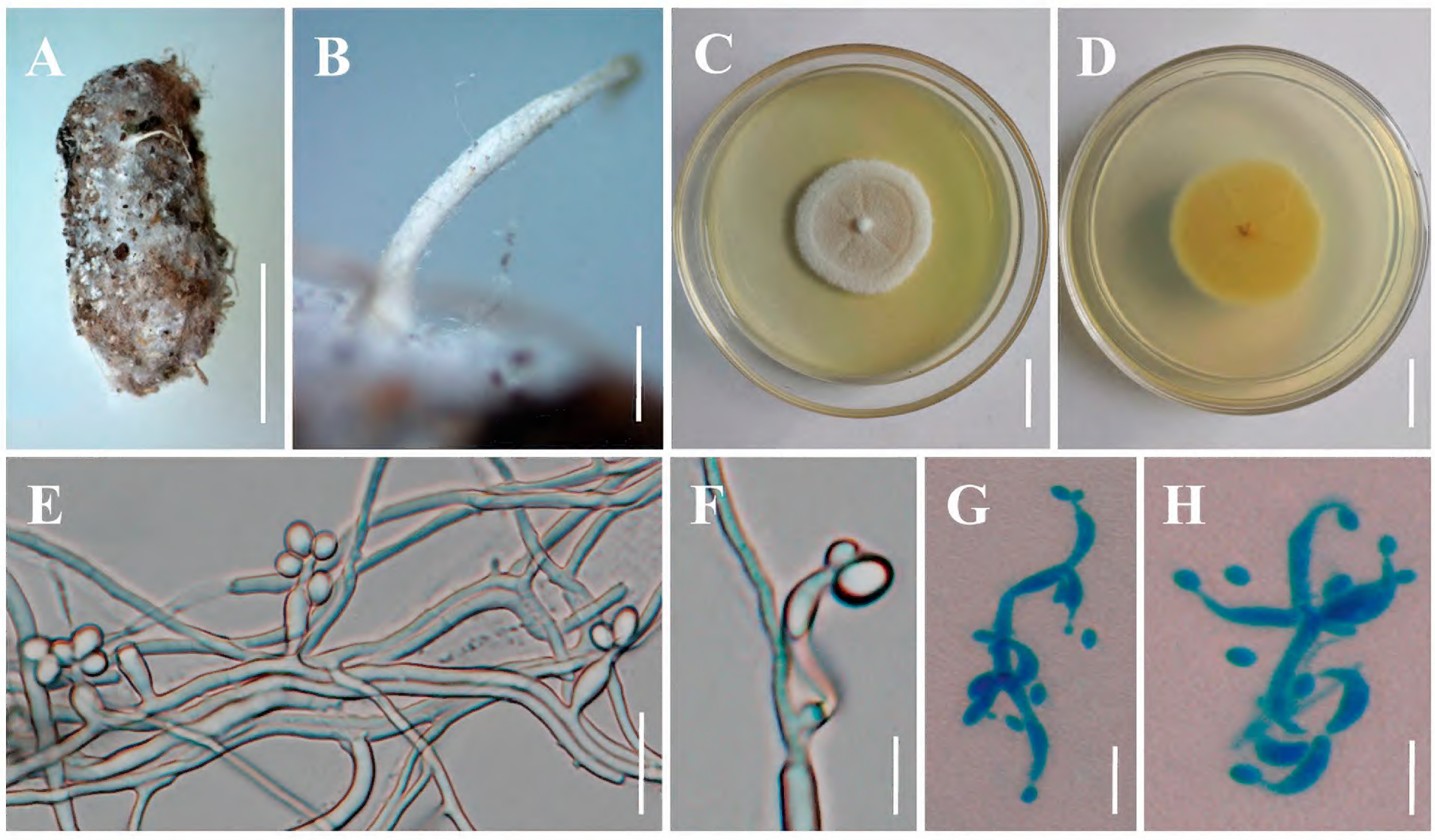

Figure 2. Morphology of *Amphichorda guizhouensis* **A** *A. guizhouensis* on bird feces **B** Synnemata **C, D** Colony obverse and reverse on PDA medium **E–H** Conidiophores, conidiogenous cells and conidia. Scale bars: 5 mm (**A**); 400 µm (**B**); 20 mm (**C–D**); 10 µm (**E, G, H**); 5 µm (**F**).

Substrate. Animal feces.

Distribution. At present, known only in Anshun City, Guizhou Province, China.

Notes. Phylogenetic analyses placed *A. guizhouensis* within the *Amphichorda* clade, forming a sister lineage to *A. felina* and *A. yunnanensis* with strong statistical support (BS/BS/PP = 97%/100%/1; Fig. 1). The species formed a distinct monophyletic group comprising two sampled strains, demonstrating significant genetic divergence from *A. felina* and *A. yunnanensis*. Morphologically, our observations unearthed distinct disparities among the three species. Specifically, *A. felina* exhibited phialides that were consistently flask-shaped, while *A. guizhouensis* featured phialides that were either cylindrical or flask-shaped. In contrast, *A. yunnanensis* possessed phialides ranging from ampulliform to flask-shaped. A particularly notable characteristic of *A. guizhouensis* was its relatively elongated phialides (6.0–20.8 × 1.8–3.7 µm). This unique morphological trait served as a crucial diagnostic feature, enabling clear differentiation of *A. guizhouensis* from other species within the *Amphichorda* genus (see Table 2).

Table 2. Hosts/substrates and asexual morphology of *Amphichorda*.

Species	Host/Substrate	Conidiophores	Phialides (µm)	Conidia (µm)	References
Amphichorda cavernicola	Bird feces; soil; plant debris; animal feces; bat guano	Cylindrical, straight or slightly curved, occasionally branched	Fusiform or ellipsoidal, straight or irregularly bent, 4.5–8.0 × 2.0–3.0	Broadly ellipsoidal to subglobose, 2.5–4.0 × 2.0–3.5	Zhang et al. 2020
Amphichorda coprophila	Chipmunk, rabbit and porcupine dung	Straight or flexuous, unbranched, bearing lateral or terminal conidiogenous cells, arranged singly or in whorls	Flask-shaped, usually with a strongly bent neck, 6–10 × 2–2.5	Subglobose to somewhat ellipsoidal, 3.5–5.5 × 2–3	Guerra-Mateo et al. 2023
Amphichorda excrementa	Animal feces	Cylindrical, straight or slightly curved, occasionally branched	Occasionally solitary, mostly in whorls of 2–3, basal portion cylindrical or flask-shaped, usually curved, 4.1–13.9 × 1.3–2.1	Globose to elliptical 1.7–3.0 × 1.2–2.5	Wang et al. 2024
Amphichorda felina	Pupae of *Anaitis efformata*; rabbit dung; moudy leaves; porcupine dung; cat dung	Straight	Solitarily or in small groups, consisting of a swollen, flask-shaped or curved, occasionally elongate basal part, 1.5–8.5 × 1.8–2.9	Subglobose, ellipsoidal or ovoidal, sometimes with a pointed base, 2.5–4.7 × 2–3.5	Wang et al. 2024
Amphichorda guana	Bat guano	Straight or slightly curved	Fusiform or ellipsoidal, straight or irregularly bent, 7–10 × 2–3	Broadly ellipsoid to subglobose, 4.5–5.5 × 3.5–5	Zhang et al. 2017
Amphichorda guizhouensis	**Animal feces**	**Cylindrical, straight or slightly curved, occasionally branched**	**Basal portion cylindrical or flask-shaped, erect or irregularly curved, tapering abruptly towards the apex, 6.0–20.8 × 1.8–3.7**	**Subglobose to ellipsoidal, 2.6–4.0 × 1.8–2.6**	**In this study**
Amphichorda kunmingensis	Animal feces	-	Solitary, occasionally in simple whorls, basal portion cylindrical or fusiform, straight or irregularly bent, 6.1–17.5 × 1.4–2.9	Globose to elliptical 2.3–4.2 × 1.6–3.0	Wang et al. 2024
Amphichorda littoralis	Sediments; fragment of floating rubber tire	Straight or flexuous, commonly unbranched, bearing lateral or terminal conidiogenous cells, arranged singly or in whorls of 2–4	Flask-shaped, usually with a strongly bent neck, 6–10 (–11.5) × 1.5–2	Subglobose, 3–4 × 2.5–3	Guerra-Mateo et al. 2023
Amphichorda monjolensis	On PDA plate consumed by an insect	Cylindrical, bearing one or more conidiogenous cells, straight or slightly bent, solitary or synnematous, sometimes branched	Flask-shaped, straight or irregularly bent, 3.1–6.1 × 2.7–5.1	Holoblastic, 2.8–3.7 × 1.8–2.9	Leão et al. 2024
Amphichorda yunnanensis	Wing surfaces of *Rhinolophus*	Cylindrical, straight or slightly curved, branched	Monoblastic to polyblastic, ampulliform to flask-shaped, 4–12 × 1–4	Globose to oval, slightly ellipsoid, 2–5 × 2–4	Liu et al. 2023

***Ovicillium pseudoattenuatum* Y. Wang & D.X. Tang, sp. nov.**
MycoBank No: 857726
Fig. 3

Etymology: "*Pseudoattenuatum*" refers to morphologically resembling *Ovicillium attenuatum*, but phylogenetically distinct.

Type. Laos • Vientiane City, Mekong Riverside Park (17.96°N, 102.60°E, 674 m above sea level), from soil on the forest floor, 11 August 2024, Yao Wang (holotype as dried culture GMB 3007); ex-type culture GMBC 3007.

Description. Sexual morph: Undetermined. **Asexual morph:** Colonies on PDA reaching 23–25 mm in diameter in 7 days at 25 °C, white to pinkish; reverse yellowish. ***Hyphae*** branched, smooth-walled, septate, hyaline, 1.2–2.8 µm wide. ***Conidiophores*** hyaline, smooth-walled, with single phialide or whorls of 2–5 phialides or verticillium-like directly from hyphae, up to 500 µm long. Phialides terminal or lateral, straight, somewhat inflated base, attenuated from the middle, sometimes undulated near the tip, 16.0–37.5 × 1.5–2.4 ($\bar{X}$ = 26.8 × 2.0, n = 50) µm. ***Conidia*** smooth-walled, hyaline, ellipsoidal to cylindrical, 3.2–4.0 × 1.7–3.2 ($\bar{X}$ = 3.7 × 2.3, n = 50) µm, aggregated in large globose to subglobose heads. Crystals absent. ***Chlamydospores*** absent.

Other material examined. Laos • Oudomxay Province, Muang Xay District, Nam Kat Yorla Pa Resort (20.71°N, 102.11°E, 708 m above sea level), from soil on the forest floor, 14 August 2024, Yao Wang (living culture GMBC 3008).

Substrate. Soil.

Distribution. Laos.

Notes. *Ovicillium pseudoattenuatum*, isolated from forest floor soil, forms a distinct phylogenetic lineage within the *Ovicillium* genus. Multilocus phylogenetic analyses reveal its close relationship with *O. attenuatum* and *O. sinense*, supported by strong statistical values (BS_{IQ}/BS_{RAx}/PP = 82%/79%/0.93). Morphologically, while sharing the characteristic undulated phialide tips with *O. attenuatum*, *O. pseudoattenuatum* differs significantly in microscopic dimensions: it possesses smaller phialides (16.0–37.5 × 1.5–2.4 µm vs 25–50 × 1.7–3.3 µm) and more compact conidia (3.2–4.0 × 1.7–3.2 µm vs 3.5–5 × 2.5–3.8 µm). Distinct from *O. sinense*, which exhibits even smaller reproductive structures (phialides 16.2–25.8 × 1.7–2.4 µm; conidia 2.1–2.9 × 1.1–1.7 µm), *O. pseudoattenuatum* is further characterized by its unique ellipsoidal to cylindrical conidial morphology, a diagnostic feature distinguishing it from all known *Ovicillium* species (Table 3).

Discussion

Amphichorda species exhibit exceptional ecological plasticity, colonizing diverse substrates including caves, marine sediments, soil, animal waste, and even biotic surfaces such as the wings of bats (*Rhinolophus* spp.). Although their primary niche is coprophilous (dung-associated)—evidenced by the recent discovery of *A. guizhouensis* and most congeners in animal excrement—their adaptability is further exemplified by colonization of specialized microhabitats. For instance, *A. felina* has been isolated from decomposing leaves and *Anaitis efformata* pupae (de Hoog 1972; Wang et al. 2024), while *A. yunnanensis* inhabits bat wing surfaces (Liu et al. 2023). Notably, three *Hapsidospora* species (*H. globosa*, *H. inversa*, and

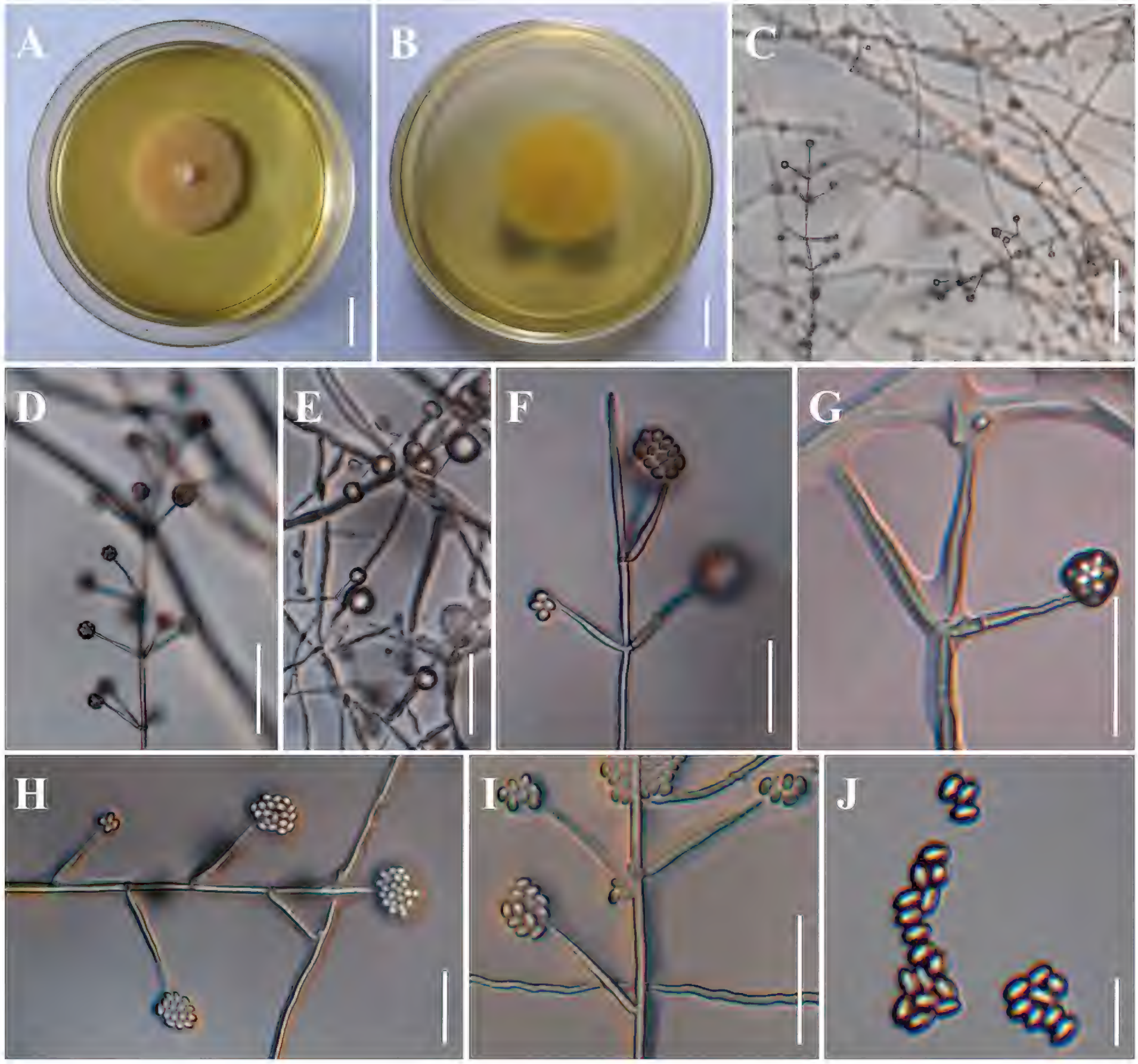

Figure 3. Morphology of *Ovicillium pseudoattenuatum* **A, B** Colony obverse and reverse on PDA medium **C–I** Conidiophores, phialides and conidia **J** Conidia. Scale bars: 10 mm (**A–B**); 100 µm (**C**); 50 µm (**D–E**); 25 µm (**F–I**); 10 µm (**J**).

H. stercoraria) also exhibit obligate coprophily. This parallel ecological specialization between *Amphichorda* and *Hapsidospora* underscores their phylogenetic affinity, suggesting either a shared ancestral adaptation to fecal substrates or convergent niche evolution within the Bionectriaceae family.

The broad ecological range of *Amphichorda* is accompanied by subtle morphological distinctions, complicating taxonomic differentiation among cryptic species. Consequently, molecular data play a pivotal role in delineating species boundaries. Recent studies have employed multi-locus sequence data (ITS, nrSSU, nrLSU, *tef1α*, *rpb1*, and *rpb2*) to resolve phylogenetic relationships within the genus (Zhang et al. 2017, 2020; Guerra-Mateo et al. 2023; Liu et al. 2023; Leão et al. 2024; Wang et al. 2024). However, GenBank records (https://www.ncbi.nlm.nih.gov, accessed 20 February 2025) remain incomplete for nrSSU, *rpb1*, and *rpb2* in this group. To address this gap, we generated comprehensive molecular datasets from five distinct *Amphichorda* species. These data enrich

Table 3. Hosts/substrates and asexual morphology of *Ovicillium*.

Species	Host/ Substrate	Conidiophores (µm)	Phialides (µm)	Conidia (µm)	Crystals	Chlamydospores (µm)	References
Ovicillium asperulatum (Synonym: *O. napiforme*)	Soil; wood of *Sorbus aria*	Simple or mostly branched, bearing whorls of 2–4 phialides, up to 105 long, with cell walls usually thicker than those of the vegetative hyphae	Straight or slightly bent, acicular, 28–68 long, 1–2 wide at the base, with minute collarette and distinct periclinal thickening at the apex	Globose, 3–4(–5) diameter, chromophilic	Absent	Abundant, subglobose or oval, 5–10 × 5–9	Giraldo et al. 2012; Zare and Gams 2016
Ovicillium attenuatum	*Auricularia* sp.	Erect, 150–500 tall, with cyanophilic encrustation, usually with whorls, but sometimes also solitary phialides	Aculeate, attenuated from the middle, mostly undulated near the tip, rather cyanophilic, measuring 25–50 × 1.7–3.3	Oval to subglobose, strongly cyanophilic, measuring 3.5–5 × 2.5–3.8, aggregated in large globose to subglobose heads	Absent	Absent	Zare and Gams 2016
Ovicillium oosporum	*Theobroma gileri*	Erect, solitary and verticillate, with slightly pigmented base producing solitary or verticillate phialides of up to five per node	Verticillate, measuring 20–50 × 1.2–2.2	Subglobose, oval to broadly oval, in some strains with a basal protrusion, cyanophilic, measuring 4–6 × 2.5–4	Absent	Present or absent	Zare and Gams 2016
Ovicillium pseudoattenuatum	**Soil**	**Single phialide or whorls of 2–5 phialides or verticillium-like directly from hyphae, up to 500 long**	**Straight, somewhat inflated base, attenuated from the middle, sometimes undulated near the tip, 16.0–37.5 × 1.5–2.4**	**Ellipsoidal to cylindrical, 3.2–4.0 × 1.7–3.2, aggregated in large globose to subglobose heads**	**Absent**	**Absent**	**In this study**
Ovicillium sinense	Pupa (Lepidoptera)	Single phialide or whorls of 2–5 phialides or verticillium-like, 17.0–21.7 × 2.3–3.0	Cylindrical, somewhat inflated base, 16.2–25.8 × 1.7–2.4, tapering to a thin neck	Globose to ovoid, 2.1–2.9 × 1.1–1.7, aggregated in large globose to subglobose heads	–	–	Chen et al. 2024
Ovicillium subglobosum	Soil	Erect, solitary and verticillate with up to four phialides per node	Measuring 25–55 × 1.5–2.2, producing conidia in large globose heads.	Subglobose with an inconspicuous protrusion at the base, rather cyanophilic, measuring 3.5–5.5 × 3.5–4.5	Absent	Absent	Zare and Gams 2016
Ovicillium variecolor	Soil	Erect, mostly branched, bearing whorls of 2–5 phialides, up to 290 long, with walls usually thicker than those of the vegetative hyphae	Straight, acicular, 18–95 long, 1–2 wide at the base, with periclinal thickening at the apex, collarette inconspicuous; some phialidic conidiogenous cells without a basal septum (adelophialides)	Subglobose or ovoid, 3–4(–5) × 2–4, slightly apiculate base, chromophilic, arranged in slimy heads	–	Absent	Giraldo et al. 2012

existing genomic resources and enhance the resolution of phylogenetic reconstructions, providing deeper insights into the evolutionary history of the genus.

Our multi-locus phylogeny (nrSSU-ITS-nrLSU-*tef1α-rpb1-rpb2*) revealed a close genetic relationship among *Amphichorda*, *Hapsidospora*, *Ovicillium*, *Proxiovicillium*, and *Bulbithecium*. Consistent with Leão et al. (2024), *Amphichorda* and *Hapsidospora* form a well-supported sister clade within Bionectriaceae (BS_{IQ}/BS_{RAx}/PP = 93%/99%/1; Fig. 1). Additionally, *Ovicillium* clustered with *Proxiovicillium* + *Bulbithecium* as a distinct lineage, while maintaining a close genetic affinity with *Amphichorda*. Although earlier studies positioned *Ovicillium* as sister to *Proxiovicillium* (Hou et al. 2023; Leão et al. 2024), our expanded sampling of seven *Ovicillium* species [compared to two in Hou et al. (2023) and three in Leão et al. (2024)] yielded more stable topological relationships among these genera. Morphological traits further corroborate these genetic linkages: *Ovicillium* species produce large globose conidial heads, *Proxiovicillium* forms conidia in elongated chains, and *Bulbithecium* exhibits slimy conidial heads arranged in chains.

The ongoing discovery of new species in biodiversity studies is essential to our comprehension of the complexity of ecosystems and the development of life. The discovery of novel species remains pivotal for elucidating ecosystem complexity and evolutionary trajectories. Here, we propose two new species—*A. guizhouensis* (isolated from animal feces) and *O. pseudoattenuatum* (from soil)—based on integrated morphological and phylogenetic evidence. A comparative analysis of morphological traits across all *Amphichorda* and *Ovicillium* members was conducted to refine taxonomic boundaries. This study not only clarifies evolutionary relationships within the two genera but also advances the systematic understanding of biodiversity in Bionectriaceae.

Acknowledgments

In this section, you can acknowledge any support given which is not covered by the author contribution or funding sections. This may include administrative and technical support, or donations in kind (e.g., materials used for experiments).

Additional information

Conflict of interest

The authors have declared that no competing interests exist.

Ethical statement

No ethical statement was reported.

Funding

This research was jointly supported by the National Natural Science Foundation of China under grants [32460004] and [32200013], the High-level Innovation Talents (No. GCC[2023]048), and the Guizhou Provincial Scientific and Technologic Innovation Base (No. [2023]003).

Author contributions

All authors have contributed equally.

Author ORCIDs

Yao Wang https://orcid.org/0000-0002-1262-6700
Hui Chen https://orcid.org/0009-0008-0291-3571
AuthorName https://orcid.org/0000-0002-4333-9106

Data availability

All of the data that support the findings of this study are available in the main text.

References

Bischoff JF, Rehner SA, Humber RA (2006) *Metarhizium frigidum* sp. nov.: A cryptic species of *M. anisopliae* and a member of the *M. favoviride* complex. Mycologia 98(5): 737–745. https://doi.org/10.1080/15572536.2006.11832645

Carmichael JW, Kendrick WB, Conners IL, Sigler L (Eds) (1980) Genera of Hyphomycetes. University of Alberta Press, 396 pp.

Chen MJ, Huang B, Li ZZ, Spatafora JW (2013) Morphological and genetic characterisation of *Beauveria sinensis* sp. nov. from China. Mycotaxon 124(1): 301–308. https://doi.org/10.5248/124.301

Chen WH, Li D, Wei YJ, Liang JD, Han YF (2024) *Ovicillium sinense*, a new species from Guizhou, China. Phytotaxa 662(2): 195–200. https://doi.org/10.11646/phytotaxa.662.2.8

Darriba D, Taboada GL, Doallo R, Posada DJ (2012) ModelTest 2: More Models, New Heuristics and Parallel Computing. Nature Methods 9(8): 772. https://doi.org/10.1038/nmeth.2109

de Hoog GS (1972) The genera *Beauveria*, *Isaria*, *Tritirachium* and *Acrodontium* gen. nov. Studies in Mycology 1: 1–41.

Fries EM (1825) Systema Orbis Vegetabilis: Primas Lineas Novae Constructionis Periclitatur; E Typographia Academica. Lunde Volume 1.

Fries EM (1832) Systema *Mycologicum*: Sistens Fungorum Ordines, Genera et Species, Huc Usque Cognitas, Quas ad Normam Methodi Naturalis Determinavit; Sumtibus Ernesti Mauritii: Gryphiswaldia. Germany Volume 3.

Giraldo A, Gene J, Cano J, de Hoog S, Guarro J (2012) Two new species of *Acremonium* from Spanish soils. Mycologia 104(6): 1456–1465. https://doi.org/10.3852/11-402

Guerra-Mateo D, Gené J, Baulin V, Cano-Lira JF (2023) Phylogeny and taxonomy of the genus *Amphichorda* (Bionectriaceae): An update on *Beauveria*-like strains and description of a novel species from marine sediments. Diversity 15(7): 795. https://doi.org/10.3390/d15070795

Hoang DT, Chernomor O, von Haeseler A, Minh BQ, Vinh LS (2017) UFBoot2: Improving the ultrafast bootstrap approximation. Molecular Biology and Evolution 35(2): 518–522. https://doi.org/10.1093/molbev/msx281

Hodge KT, Gams W, Samson RA, Korf RP, Seifert KA (2005) Lectotypification and status of *Isaria* Pers. Taxon 54(2): 485–489. https://doi.org/10.2307/25065379

Hopple JS (1994) Phylogenetic investigations in the genus *Coprinus* based on morphological and molecular characters. Ph.D. Dissertation, Duke University, Durham, NC, USA.

Hou LW, Giraldo A, Groenewald JZ, Rämä T, Summerbell RC, Huang GZ, Cai L, Crous PW (2023) Redisposition of acremonium-like fungi in Hypocreales. Studies in Mycology 105(1): 23–203. https://doi.org/10.3114/sim.2023.105.02

Kalyaanamoorthy S, Minh BQ, Wong TKF, von Haeseler A, Jermiin LS (2017) ModelFinder: Fast model selection for accurate phylogenetic estimates. Nature Methods 14(6): 587–589. https://doi.org/10.1038/nmeth.4285

Leão AF, Condé TO, Dutra YLG, Rosado AWC, Grazziotti PH, Neves SC, Fraga LMS, Kasuya MCM, Pereira OL (2024) *Amphichorda monjolensis* sp. nov., a new fungal species isolated from a Brazilian limestone cave, with an update on *acremonium*-like species in Bionectriaceae. Brazilian Journal of Microbiology 55(2): 1569–1585. https://doi.org/10.1007/s42770-024-01289-y

Lechat C, Fournier J (2019) New insights into *Stilbocrea* (Hypocreales, Bionectriaceae): Recognition of *S. colubrensis*, a new species from Martinique (French West Indies), and observations on lifestyle and synnematous asexual morphs of *S. gracilipes* and *S. macrostoma*. Ascomycete.Org : Revue Internationale pour la Taxinomie des Ascomycota 11(6): 183–190. https://doi.org/10.25664/ART-0272

Liu ZY, Liang ZQ, Whalley AJS, Yao YJ, Liu AY (2001) *Cordyceps brittlebankisoides*, a new pathogen of grubs and its anamorph, *Metarhizium anisopliae* var. majus. Journal of Invertebrate Pathology 78(3): 178–182. https://doi.org/10.1006/jipa.2001.5039

Liu XF, Tibpromma S, Hughes AC, Chethana KWT, Wijayawardene NN, Dai DQ, Du TY, Elgorban AM, Stephenson SL, Suwannarach N, Xu JC, Lu L, Xu RF, Maharachchikum-

bura SSN, Zhao CL, Bhat DJ, Sun YM, Karunarathna SC, Mortimer PE (2023) Culturable mycota on bats in central and southern Yunnan Province, China. Mycosphere : Journal of Fungal Biology 14(1): 497–662. https://doi.org/10.5943/mycosphere/14/1/7

Minh BQ, Schmidt HA, Chernomor O, Schrempf D, Woodhams MD, von Haeseler A, Lanfear R (2020) IQ-TREE 2: New models and efficient methods for phylogenetic inference in the genomic era. Molecular Biology and Evolution 37(5): 1530–1534. https://doi.org/10.1093/molbev/msaa015

Rehner SA, Buckley EA (2005) *Beauveria* phylogeny inferred from nuclear ITS and *EF1-α* sequences: Evidence for cryptic diversification and links to *Cordyceps* teleomorphs. Mycologia 97(1): 84–98. https://doi.org/10.3852/mycologia.97.1.84

Rehner SA, Minnis AM, Sung GH, Luangsa-ard JJ, Devotto L, Humber RA (2011) Phylogeny and systematics of the anamorphic, entomopathogenic genus *Beauveria*. Mycologia 103(5): 1055–1073. https://doi.org/10.3852/10-302

Ronquist F, Teslenko M, van der Mark P, Ayres DL, Darling A, Höhna S, Larget B, Liu L, Suchard MA, Huelsenbeck JP (2012) MrBayes 3.2: Efficient Bayesian phylogenetic inference and model choice across a large model space. Systematic Biology 61(3): 539–542. https://doi.org/10.1093/sysbio/sys029

Spatafora JW, Sung GH, Sung JM, Hywel-Jones NL, White Jr JF (2007) Phylogenetic evidence for an animal pathogen origin of ergot and the grass endophytes. Molecular Ecology 16(8): 1701–1711. https://doi.org/10.1111/j.1365-294X.2007.03225.x

Stamatakis A, Hoover P, Rougemont J (2008) A rapid bootstrap algorithm for the RAxML Web servers. Systematic Biology 57(5): 758–771. https://doi.org/10.1080/10635150802429642

Sung GH, Hywel-Jones NL, Sung JM, Luangsa-ard JJ, Shrestha B, Spatafora JW (2007) Phylogenetic classification of *Cordyceps* and the clavicipitaceous fungi. Studies in Mycology 57: 5–59. https://doi.org/10.3114/sim.2007.57.01

Vilgalys R, Hester M (1990) Rapid genetic identification and mapping of enzymatically amplified ribosomal DNA from several *Cryptococcus* species. Journal of Bacteriology 172(8): 4238–4246. https://doi.org/10.1128/jb.172.8.4238-4246.1990

Voglmayr H, Jaklitsch WM (2019) *Stilbocrea walteri* sp. nov., an unusual species of Bionectriaceae. Mycological Progress 18(1): 91–105. https://doi.org/10.1007/s11557-018-1427-0

Wang Y, Tang DX, Luo R, Wang YB, Thanarut C, Dao VM, Yu H (2023) Phylogeny and systematics of the genus *Clonostachys*. Frontiers in Microbiology 14: 1117753. https://doi.org/10.3389/fmicb.2023.1117753

Wang ZQ, Zhao J, Dong QY, Wang Y, Lu YL, Luo R, Yu H (2024) Multi-locus molecular phylogenetic analysis reveals two new species of *Amphichorda* (Bionectriaceae, Hypocreales). MycoKeys 106: 287–301. https://doi.org/10.3897/mycokeys.106.117205

White TJ, Bruns TD, Lee SB, Taylor JW (1990) Amplifcation and direct sequencing of fungal ribosomal RNA genes for phylogenetics. In: Innis MA, Gelfand DH, Sninsky JJ, White TJ (Eds) PCR protocols: a guide to methods and applications. Academic Пресс, 315–322. https://doi.org/10.1016/B978-0-12-372180-8.50042-1

Zare R, Gams W (2016) More white verticillium-like anamorphs with erect conidiophores. Mycological Progress 15(10–11): 993–1030. https://doi.org/10.1007/s11557-016-1214-8

Zhang ZF, Liu F, Zhou X, Liu XZ, Liu SJ, Cai L (2017) Culturable mycobiota from Karst caves in China, with descriptions of 20 new species. Persoonia 39(1): 1–31. https://doi.org/10.3767/persoonia.2017.39.01

Zhang ZF, Zhou SY, Eurwilaichitr L, Ingsriswang S, Raza M, Chen Q, Zhao P, Liu F, Cai L (2020) Culturable mycobiota from Karst caves in China II, with descriptions of 33 new species. Fungal Diversity 106(1): 29–136. https://doi.org/10.1007/s13225-020-00453-7